Sustainable Energy Technologies and Assessments 42 (2020) 100820

Contents lists available at ScienceDirect

Sustainable Energy Technologies and Assessments

journal homepage: www.elsevier.com/locate/seta

Original article

Influence of co-depositor materials and modification of substrate on the formation of dendrites on the anode of a zinc-based secondary battery

Bart Homan[a,c,*], Diego F. Quintero Pulido[b,c], Marnix V. ten Kortenaar[c], Johann L. Hurink[a], Gerard J.M. Smit[a]

[a] Computer Architecture for Embedded Systems, University of Twente, Enschede, the Netherlands
[b] Department of Sanitary and Environmental Engineering, La Salle University, Bogotá, Colombia
[c] Dr Ten B.V., Wezep, the Netherlands

ARTICLE INFO

Keywords:
Dendrites
Zinc
Graphite
Anode
Deposition

ABSTRACT

Dendrite formation poses serious problems in the operation of zinc-based batteries. Electrode material and electrolyte composition are known to have an influence on the dendrite formation. In this paper possible solutions for the reduction of dendrite formation at the anode of a zinc-based battery are studied. The electrochemical behaviour of various electrode materials and electrolyte compositions is researched. It is observed that the tested electrode materials have no significant impact on the reaction at the anode. However, significant reduction in dendrite formation are observed at various electrode materials. The largest reduction in dendrite formation is observed when SGL bipolar graphite is used as electrode material. Furthermore, using several analysis methods (CV, EIS, SEM) it is observed that the addition of low concentrations (around 10% of the main component concentration) of certain additives ($MgBr_2$, $MnSO_4$) to the electrolyte has no significant impact on the electrolyte reaction at the anode, but prevents the formation of dendrites. Finally, the changes in substrate material and electrolyte additive do not have significant influence on the over-all performance of the battery.

Introduction

Batteries get more and more an important part of future energy systems [1]. They are for example used to store electricity generated by photovoltaic panels during the day for usage during the evening or night, resulting in peak-shaving and reduced stress on the electrical grid [2]. Next to the grid support aspect, also economic advantages can be achieved by storing electricity at times when it is cheap for usage at times when it is expensive. Another example for using a battery is its possibility to function as back-up in emergency situations. For all those applications different batteries can be considered, like e.g. lead-acid batteries and lithium-ion batteries, which all have their strong points and drawbacks [3]. An alternative battery that could be used in future energy systems is the zinc-based battery. Zinc-based batteries have some advantages. On the one hand most components used for zinc-based batteries, (e.g. zinc, zinc–halogen salts, graphite) are abundant and readily available [4–6] and therefore relatively cheap. On the other hand the aforementioned components used in zinc-based batteries present only mild health-risks and are moderatly hazardous to the environment [7], as opposed to e.g. the components used in lead-acid batteries [8,9].

The zinc-based primary battery (i.e. not rechargeable) has been a fixture in the world of energy storage since the 1970's [10,11]. Although the research into zinc-based secondary batteries (i.e. rechargeable) is an ongoing process, no definitive zinc-based secondary battery technology has emerged yet. One such technology, currently under development at Dr. Ten B.V., is the *Seasalt battery* [12,13]. A particular challenge in the development of the *Seasalt battery* (or zinc-based secondary batteries in general) is the formation of dendrites at the anode [10,14]. The formation of dendrites at the anode may accellerate ageing[1], cause reduced storage capacity and short-circuiting of the battery [15]. An example of dendrites formed during testing of a $ZnBr_2$ based electrochemical cell is shown in Fig. 1. In this case the deposited zinc forms a brittle "Christmas tree"-like structure at the anode. If this structure continues to grow, eventually it could reach the cathode, causing a short-circuit. Furthermore, if these structure fractures from the anode, the broken part no longer takes part in the electrochemical reaction and as a result the cell-capacity is diminished.

* Corresponding author at: Computer Architecture for Embedded Systems, University of Twente, Enschede, the Netherlands.
E-mail address: b.homan@utwente.nl (B. Homan).

[1] Gradual performance degradation of a battery, caused by complex interrelated phenomena that depend on battery chemistry, design, environment, and the actual operational conditions [15]

https://doi.org/10.1016/j.seta.2020.100820
Received 25 February 2020; Received in revised form 3 June 2020; Accepted 4 September 2020

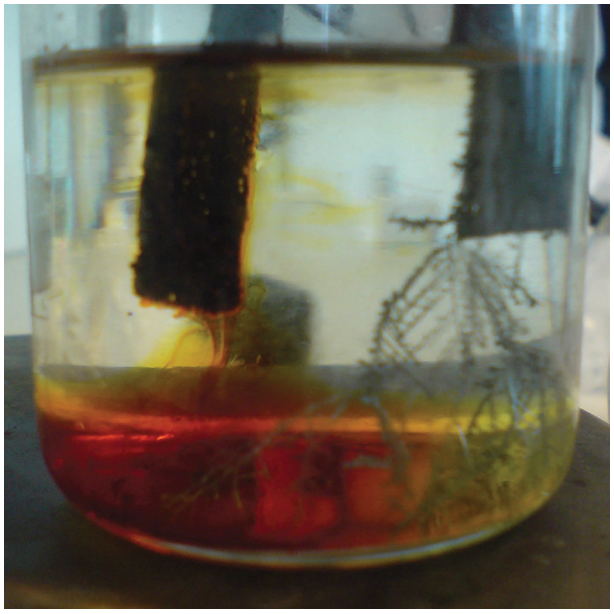

Fig. 1. The formation of dendrites on the anode of a *Seasalt Battery* (i.e. a zinc based battery).

The deposition behavior is susceptible to changes in various conditions like pH, temperature and current density [16,17], and can be influenced using various techniques. Fukami et al. [18,19] report that the application of electrochemical oscillations during zinc deposition yields wafer-like structures rather than dendrites. Shitanda et al. [20] report that creating a dot-pattern on the substrate surface at the nano-level yields dendrites only where the dots are located on the substrate surface, while Koda et al. [21] note that dendrite formation can be suppressed if deposition takes place within nanopores of a given substrate. Gomes et al. [22,23] state that by the addition of certain surfactants it is possible to deposit zinc with a different preferred orientation, crystal shape (needles, pyramids, cauliflowers) and size. However, these solutions are impractical for application in a battery because they would either increase the costs of such a battery dramatically, or severely influence the overall behaviour of the battery (e.i. the progression of voltage and current during charging and discharging, the *Open Circuit Potential*, etc.). Thus different, more practical means of influencing the deposition behaviour have to be applied.

The influence of the substrate on the deposition behavior of zinc has been studied widely. Various substrate materials such as steel [24], platinum [25], magnesium [26], titanium [27], glassy carbon and graphite [28] have been researched. The common conclusion in these studies is that the composition of the substrate is of vital importance to the zinc-deposition behavior. It is also concluded that the surface preparation of a substrate can influence the zinc deposition behavior [29].

The addition of a second depositing material, or co-depositor is also known to have an effect on the deposition of zinc. The co-depositor material should "interfere" with the normal crystallization process of zinc in such a way that structures other than dendrites are formed during deposition. In this case, the cation of the co-depositor is built into the crystal structure made up by the Zn^{2+} ions altering the overall crystal structure. Several compounds with various cations suitable for co-deposition with zinc have already been tested and described; e.g. manganese [30], nickel, cobalt, iron [31,32], copper [33], and calcium [34]. The effects of polar additives acetonitrile, ethylenediamine and ammonia were explored by Abbott et al. [35], while the effects of various organic additives have been researched by Li et al. [36] and Ortiz et al. [37]. Our preliminary investigation of the behaviour of various additives, reproducing and adapting experiments described in [31–37], however, did not yield satisfactory results. We found that compounds containing nickel or aluminium severely reduced the deposition reaction on the anode, thereby reducing the energy storage capacity. Furthermore, we observed that compounds containing calcium limited the reversibility of the deposition at the anode, reducing the charge/discharge cycle-life. Moreover, we observed that compounds containing iron or polar additives negatively influenced the reactions at the cathode. However, additives containing manganese or magnesium showed the most promising results, as these were observed to have only limited influence on the reactions at the electrodes.

In this work possible solutions to the problem of dendrite formation at the cathode of a zinc-based secondary battery are explored. Firstly, in Section "Materials and methods" the used methods and techniques are outlined and in SubSection "Reference condition" a reference condition to which the results of all subsequent experiments are compared, is given. In Section "Results and discussion" the main results of this research are discussed. Firstly, in SubSection "Influence of various substrates" the influence of various substrates on the dendrite formation is considered and secondly, in SubSection "Influence of various additives" the influence of several additives containing magnesium and manganese ions, that were observed to have little influence on the reaction at the electrodes, is investigated. Finally, in SubSection "Combined improvements" the optimal combination of substrate and additive is explored, the surface of the deposited zinc layers is analysed using *Scanning Electron Microscopy* (SEM) and the difference in electrochemical behaviour between the reference condition and the optimal combination of substrate and additive is explored using *Electrochemical Impedance Spectroscopy*. The paper ends with conclusions in Section "Conclusion" and possible topics for future research in Section "Future work".

Materials and methods

The *Cyclic Voltammetry* (CV) and *Chrono-Amperomtery* (CA) experiments were conducted on a *Metrohm Autolab PGSTAT101* potentiostat, at room temperature and ambient pressure, using a Ag/AgCl reference electrode, obtained from the Metrohm company. All CV experiments were caried out at a scanrate of 100 mV/s. The electrode surface morphology was analyzed using a standard optical microscope. The *Scanning Electron Microscopy* (SEM) images were taken using a *JEOL 1610 LA* scanning electron microscope. The *Electrochemical Impedance Spectroscopy* (EIS) measurements were conducted using a *CH Instruments 600E* electrochemical analyser. The EIS experiments were conducted at room temperature and ambient pressure, within a Faraday cage, using a Ag/AgCl reference electrode, obtained from the Metrohm company. The SEM measurements were analysed using the *EQUIVCRT* method and software, developed by Boukamp [38,39].

In each experiment, the counter-electrode was a *standard graphite* plate while the working electrode material was varied. Both plates were partially submerged in the electrolyte, making the effective area of each electrode 1 cm^2. In all experiments, an excess of electrolyte was used to make sure that absence of electrolyte could never be the limiting factor in the deposition. Unless specifically mentioned, all chemicals ($ZnBr_2$, $MgBr_2$, $MnSO_4$, etc.) were of *trace metals basis* grade (purity 99.999%) and were obtained from the Sigma–Aldrich corporation. The electrode materials were obtained from SGL graphites SE.

Reference condition

As the main goal of this work is to achieve a reduction in dendrite formation, i.e. to show changes in zinc deposition behaviour, first the reference to which these changes or reductions are compared has to be precisely specified. All further achieved results are compared to the conditions and results of this reference experiment.

Under the conditions of the reference experiment dendrite formation occurs as shown in Fig. 1. The electrolyte used was a 1 M $ZnBr_2$ (aq) solution and this is referred to as *standard electrolyte*. The anode (or

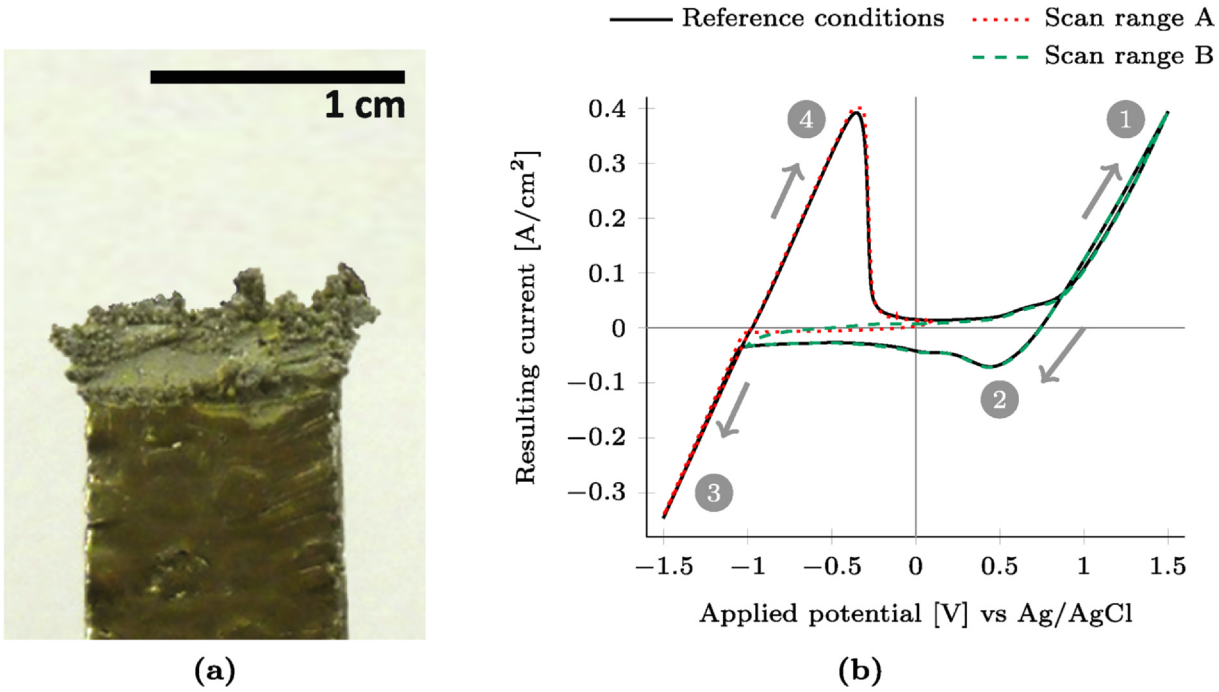

Fig. 2. (a) The morphology of a zinc layer deposited at −1.3 V for 1 h on *standard graphite* from *standard electrolyte*. (b) Voltammogram for the *reference conditions*, the numbers correspond to Eqs. (1)–(4) which describe the chemical reactions likely to occur at various points during the CV experiment.

substrate) was a graphite-coated iron film and this electrode material is referred to as *standard graphite*. The iron film is completely encased by the graphite layer, so the core never comes into contact with the electrolyte. Furthermore the experiments were conducted at atmospheric pressure and ambient temperature, with a Ag/AgCl reference electrode, these are referred to as *reference conditions*. For the deposition experiments a potential of −1.3 V was chosen, since at this potential the zinc deposition occurs sufficiently fast to be observed visually during the experiment, while gas evolution at the anode is not observed at this potential.

Results and discussion

In the following subsections the dendrite formation and the electrochemical behaviour of various substrate/electrolyte combinations is investigated. Firstly, the dendrite formation is evaluated by visual inspection of the zinc layer deposited at the anode. The deposited zinc layer of each substrate/electrolyte combination is compared to a zinc layer deposited under the *reference conditions* (see Fig. 2a). Any significant reduction in dendrite formation is considered to be an improvement.

Secondly, the electrochemical behaviour of each substrate/electrolyte combination is investigated using *cyclic voltammetry* (CV). The resulting voltammograms are compared to the *reference condition* (see Section “Reference condition”). If the differences between the voltammograms for the two cases are small, the electrochemical behaviour of the compared electrode/electrolyte combinations is similar. In this case the substrate/electrolyte combination is considered to be usable in the zinc-based secondary battery.

Analysis of the reference condition

Fig. 2b shows the voltammogram of *standard electrolyte* and *standard graphite* under the *reference conditions*. The numbers in the graph of Fig. 2b correspond to Eqs. (1)–(4), which describe the main reaction likely to take place at each step during the voltammetry experiment.

$$2Br^-(aq) \rightarrow Br_2(aq) + 2e^- \quad (1)$$

$$Br_2(aq) + 2e^- \rightarrow 2Br^-(aq) \quad (2)$$

$$Zn^{2+}(aq) + 2e^- \rightarrow Zn(s) \quad (3)$$

$$Zn(s) \rightarrow Zn^{2+}(aq) + 2e^- \quad (4)$$

Starting at 0 V and increasing the potential, i.e. following the graph in the direction of the arrows, initially the resulting current increases slowly. From ~ 0.8 V onwards, however, there is much faster increase. Here it is likely that the bromide ions in the electrolyte are oxidized, forming bromine (Eq. (1)). Note, that additional (side) reactions can also take place here, forming (intermediate) reaction products e.g. polybromide ions. These types of reactions are further explored in [12]. There is no clear peak in this part in the graph because there is an abundance of bromide ions present in the electrolyte, hence new bromide ions can always reach the electrode to react. Visually, a reddish brown liquid appears at the working electrode. No formation of oxygen bubbles is observed at the electrode, indicating that water splitting does not occur during this part of the CV experiment.

When the applied potential is lowered again, the resulting current reaches a local minimum of ~ −0.1 A/cm^2 at an applied potential of 0.5 V. Here it is likely that the bromine reacts back to bromide ions (Eq. (2)). The small negative peak indicates that not all bromine remains in the vicinity of the electrode, hence not all bromine can react back to form bromide ions. Visually, no more reddish brown liquid is formed, and part of the liquid that was already formed sinks to the bottom of the reaction vessel and remains there.

When the applied potential is lowered below −1 V the resulting current drops steeply. Here it is likely that zinc ions from the electrolyte are reduced to metallic zinc at the electrode (Eq. (3)). As before, there is no clear peak at this point in the graph. In this case it is because there is an abundance of zinc ions present in the electrolyte. Visually a silverish layer appears on the electrode, indicating the formation of a zinc-layer on the electrode. No formation of hydrogen bubbles is observed at the electrode, again indicating that water splitting does not occur during this part of the CV experiment.

When the applied potential is increased again the resulting current steeply increases, until a peak of ~0.4 A/cm^2 at an applied potential of −0.5 V is reached. Here it is likely that metallic zinc reacts to form zinc

ions (Eq. (4)). The large peak indicates that most zinc, formed in the previous step, reacts back to zinc ions. This is to be expected as the metallic zinc remains mostly on the electrode after it is created, hence it can react back to form zinc ions. Visually the silverish layer disappears from the electrode.

This CV experiment was repeated for 100 cycles and the shape of the graph remained the same. Visually, after the experiment no silverish layer remained on the electrode, however a small layer of reddish brown liquid remained at the bottom of the reaction vessel.

As during a CV experiment, the behaviour of the electrode alternates between the behaviour of a cathode (positive voltage) and anode (negative voltage) it may occur that the reaction at the cathode has an influence on the reaction at the anode and vice versa. Therefore, we also test if this is the case for *standard electrolyte* and *standard graphite* under the *reference conditions* by investigating the CV for two different scan ranges: scan range A (−1.5 V to 0.1 V), where zinc deposition is certain to occur and scan range B (−1.0 V to 1.5 V) where zinc deposition is certain not to occur. The corresponding voltammograms are shown in Fig. 2b. Both voltammograms perfectly overlap the complete voltammogram (−1.5 V to 1.5 V), thus demonstrating that the behaviour of the electrolyte at the cathode does not influence its behaviour at the anode. Therefore, in the following, the focus is on the deposition of zinc at the anode and behaviour of the cathode is considered to be boyond the scope of this work.

Influence of various substrates

To study the influence of different graphite types on the deposition of zinc at the anode, four commercially available graphite types were tested, in addition to the standard graphite described in Section “Materials and methods”, these types are:

1. Sigraflex, a flexible graphite type with an iron core[2].
2. SGL Bipolar, a smooth inflexible graphite sheet.
3. SGL felt gray, a porous graphite sheet.
4. SGL felt black, a porous graphite sheet.

In Fig. 3 the electrochemical behaviour of the graphite types is shown. It can be seen that the over-all behaviour of all graphite types is similar. Between −1.5 V and −0.5 V, (the anode side), the voltammograms for all substrates are almost identical. The largest differences in this range are in the height of the peak at −0.6 V. In the range between −1.5 V and 0.5 V larger differences are visible. The Sigraflex and SGL Bipolar substrates show very similar behaviour to the *standard graphite*. However,the SGL felt gray and SGL felt black substrates do show differences. Hence, the lower peak is located around −0.1 V while the other substrates show this peak at around 0.3 V. The peak is also significantly higher for SGL felt black and SGL felt gray substrates than for the standard graphite. These differences are most likely attributed to the physical properties of the substrate. Where the *standard graphite*, Sigraflex and SGL Bipolar substrates have smooth surfaces, while the SGL felt black and SGL felt gray substrates have porous surfaces. However, in the potential range where zinc deposition at the anode occurs, between −1.5 V and 0.5 V the behaviour of all tested substrates is similar to the standard graphite, showing that all four graphite types are potentially usable in the zinc-based battery as a replacement of the *standard graphite*.

In Fig. 4, the morphology of the zinc deposited at the anode surface, on four different substrates is shown. In all four cases, the zinc layer is deposited from *standard electrolyte* by applying a potential of −1.3 V (vs Ag/AgCl) for one hour. From visual inspection it is immediately clear that the morphology of the deposited zinc differs significantly for the various substrates. Both the SGL felt black and the SGL felt gray electrodes (Fig. 4a and b) are mostly smooth. The irregularities in the zinc layer may be attributed to the porosity of the substrate material. There are also some dendrites which are mostly needle-shaped. The Sigraflex electrode (Fig. 4c) shows broad dendrites, similar to the dendrites on the *standard graphite*. Furthermore the surface of the deposited zinc layer seems rough and cracked. The SGL bipolar electrode (Fig. 4d) shows no dendrites, meaning that the zinc is deposited as one smooth layer. However, there are some irregularities towards the interface between the area where zinc was deposited and where no zinc was deposited. The absence of dendrites is in sharp contrast with a zinc layer deposited on *standard graphite* (Fig. 2a) where dendrites are abundant.

From the cyclic voltammetry experiments and visual inspection of the electrodes, it can be concluded that:

- The electrochemical behaviour of the electrolyte at the anode is nearly identical for all four tested substrates.
- The results of the CV experiments show that all four tested substrates are a suitable replacement for the *standard graphite* electrode in a zinc-based secondary battery.
- The SGL bipolar electrode (Fig. 4d) shows the least dendrite formation, out of all tested substrates.
- The Sigraflex substrate (Fig. 4c) is both in its electrochemical behaviour and in the dendrite formation most similar to the *standard electrode*.

Influence of various additives

Our previous research on this subject (see Section “Introduction”) indicated that compounds containing magnesium or manganese may have the potential to reduce dendrite formation. Therefore we studied the influence of magnesium bromide ($MgBr_2$) and manganese sulphate ($MnSO_4$) on the deposition behaviour of zinc.

Note, that it would be more logical to use manganese bromide ($MnBr_2$) as an additive, as introducing SO_4^{2-} ions could result in unwanted side-reactions that (negatively) influence the electrochemical behaviour, whereas Br^- ions are already present (due to $ZnBr_2$) hence, no additional side reaction are likely to occur. However, preliminary studies using $MnBr_2$ showed less than promising results. Although voltammograms showed no large differences in the electrochemical behaviour, visual inspection of the anode showed that the deposited zinc layer had a rather brittle and dusty structure, which are unwanted properties for the structure of the deposited zinc-layer.

The zinc layers were deposited on a *standard graphite* electrode from 1 M $ZnBr_2$ (*standard electrolyte*) plus 0.1 M of the co-depositor material. Firstly the influence of the co-depositor on the electrochemical behaviour was studied.

In Fig. 5, the voltammograms of the zinc depositions on *standard graphite* from 1 M $ZnBr_2$ + 0.1 M of the selected co-depositors are shown in comparison to a voltammogram of zinc deposited under *reference conditions*. The voltammograms of 1 M $ZnBr_2$ + 0.1 M $MgBr_2$ and 1 M $ZnBr_2$ + 0.1 M $MnSO_4$ show only slight differences to the voltammogram of the *reference condition*. The main difference in the potential range where zinc deposition occurs (−1.5 V to −0.1 V) is in the height of the peak around −0.4 V. This peak in the voltammogram of 1 M $ZnBr_2$ + 0.1 M $MnSO_4$ is significantly lower than the peaks in the voltammograms of $MgBr_2$ and 1 M $ZnBr_2$ and of the *standard electrolyte*, so a lower current results from the same potential. This difference in electrochemical behaviour is likely to have a negative influence on the battery performance, as a lower resulting current at the anode is likely to result in a lower over-all battery current, compared to the *reference conditions*.

To determine the influence of both of the co-depositors on the deposition behaviour, a deposition test (using chrono-amperometry) was performed on a standard graphite anode and electrolytes containing the

[2] Note that the iron core is completely encased in the graphite compound, and thus is never exposed to the electrolyte

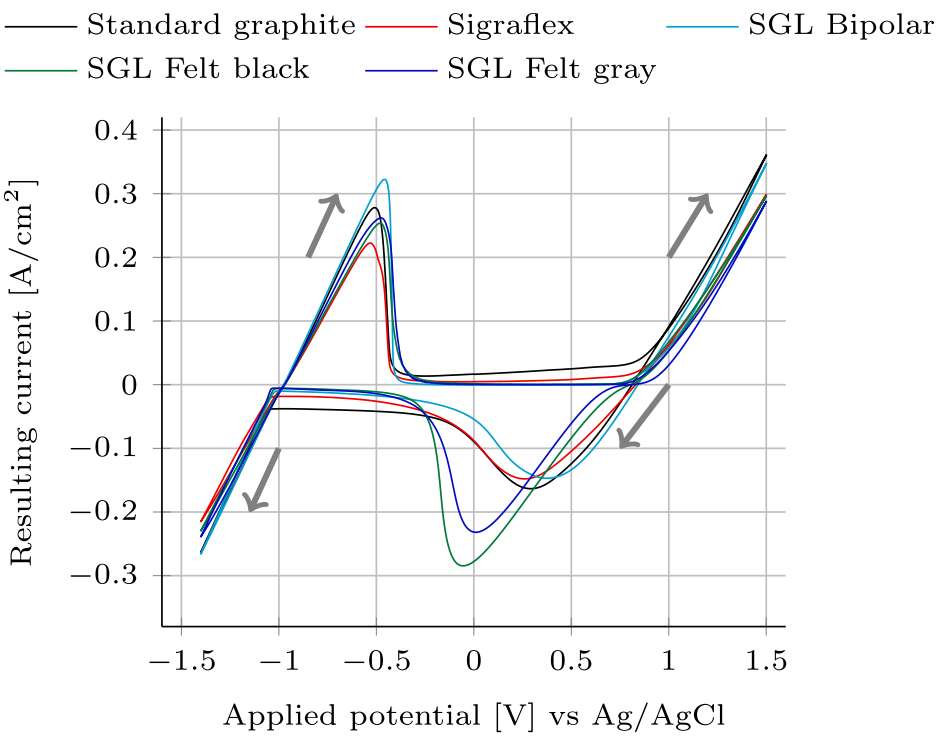

Fig. 3. Cyclic voltammogram of *standard electrolyte* for various substrates.

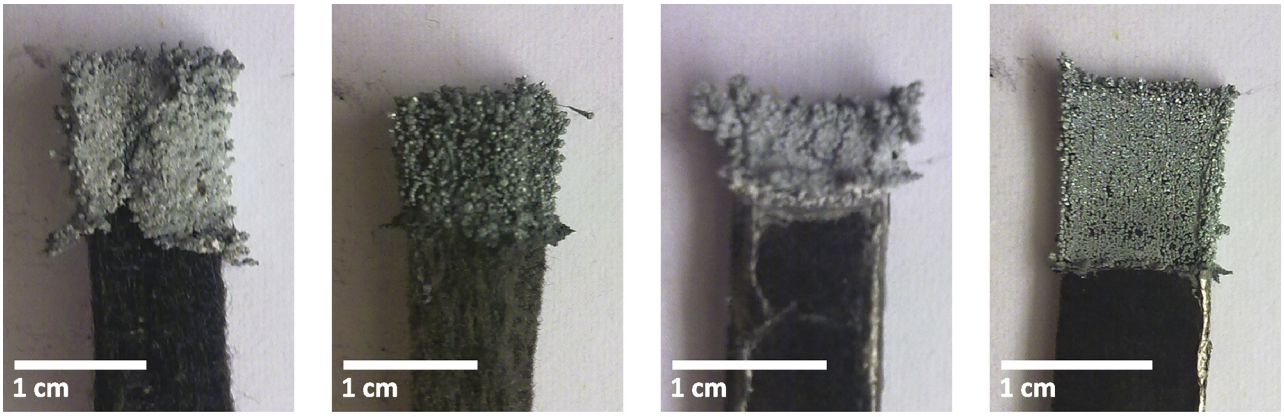

Fig. 4. Morphology of zinc deposited at −1.3 V for 1 h on varied substrates from *standard electrolyte*.

two suggested co-depositors. The zinc-layers, deposited for 1 h at −1.3 V (vs Ag/AgCl), are shown in Fig. 6. Both co-depositors are observed to have a significant influence on the behaviour of the deposition of the zinc-layer. From visual inspection it is immediately clear that neither the zinc layer deposited from 1 M $ZnBr_2$ + 0.1 M $MgBr_2$ (Fig. 6a) nor the zinc layer deposited from 1 M $ZnBr_2$ + 0.1 M $MnSO_4$ (Fig. 6c) shows significant dendrite formation. This is in sharp contrast with the dendrites formed during a deposition with 1 M $ZnBr_2$ without co-depositors (see Fig. 2a). Since the differences in the deposited zinc layers between the two electrolytes are so small, the anodes were also inspected with an optical microscope (see Fig. 6b and d). It is observed that the morphology of the zinc layers, deposited with both co-depositors, is very smooth. In particular, the zinc layer deposited from 1 M $ZnBr_2$ + 0.1 M $MgBr_2$ (Fig. 6a and b) seems evenly distributed over the anode surface and therefore is especially useful in zinc-based batteries.

In the previous experiments, a ratio of 10:1 between the depositor and the co-depositor was used. As this ratio was chosen for convenience, it still needs to be established what the optimal ratio is; i.e. where the surface of the deposited zinc layer is as smooth as possible, and where the influence of the co-depositor on the behaviour of the battery remains minimal. There should be an optimal ratio, because if the concentration of co-depositor is very low compared to the concentration of depositor, the deposition will be dominated by the depositor, and the morphology of the deposited layer will be as if there were no co-depositor present. However, if there is a high concentration of co-depositor, the morphology of the deposited layer will be similar to the characteristics of the co-depositor.

To get some insight in the optimal ratio, deposition tests were performed with electrolytes using other depositor/co-depositor ratios. In Fig. 7, the morphology of zinc layers deposited at 1.3 V for 1 h on graphite from 1 M $ZnBr_2$ and various concentrations of co-depositor is shown. From visual inspection of the zinc layers deposited from $ZnBr_2$ and $MgBr_2$ (see Fig. 7a) it is immediately clear that for co-depositor concentrations that are significantly higher and lower than 0.1 M there are significantly more dendrites formed than with a co-depositor concentration of 1 M. Therefore, as hypothesized, there seems to be an

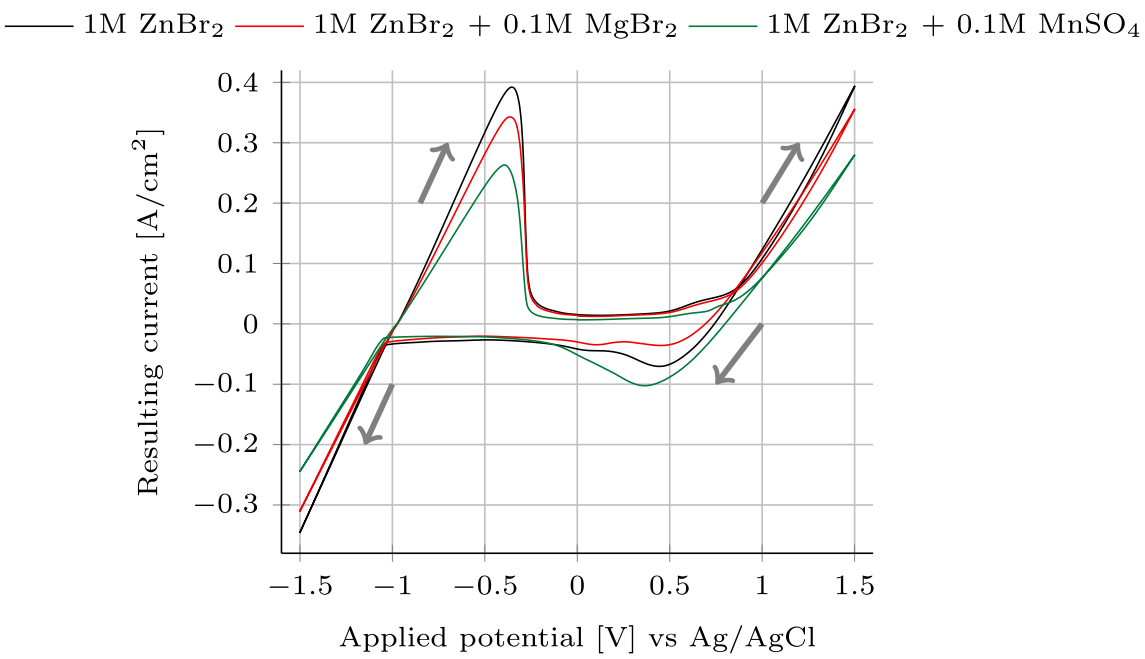

Fig. 5. Cyclic voltammogram for various electrolytes on *standard graphite*.

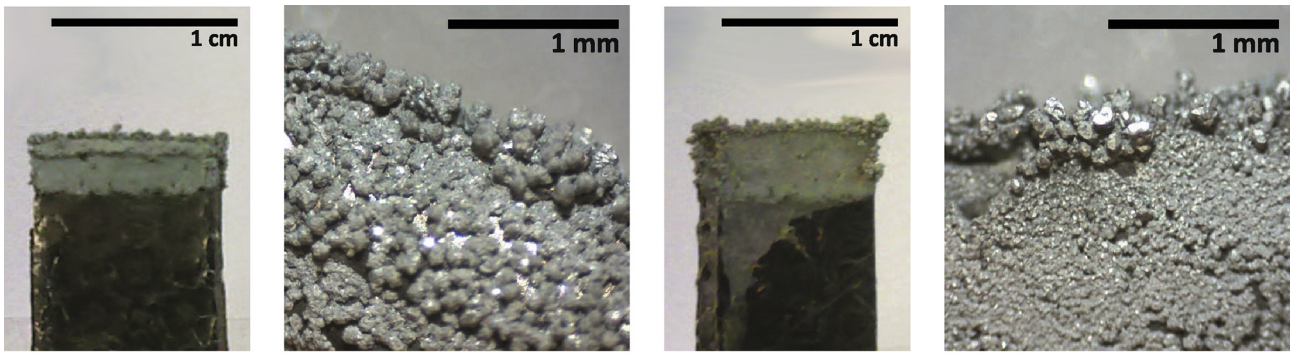

Fig. 6. Morphology of zinc deposited at −1.3 V for 1 h on *standard graphite* from 1 M $ZnBr_2$ + 0.1 M co-depositor. Pictures (b) and (d) were obtained using a standard optical microscope.

optimum concentration of co-depositor for $MgBr_2$, where the least dendrites are formed and in this case this seems to be around 0.1 M $MgBr_2$. Visual inspection of zinc layers deposited from $ZnBr_2$ and $MnSO_4$ shows similar behaviour. The optimal co-depositor concentration of $MnSO_4$ also seems to be 0.1 M.

From the cyclic voltammetry experiments and visual inspection of the electrodes, it can be concluded that:

- Out of the two tested co-depositors, an electrolyte with 0.1 M $MgBr_2$ as co-depositor behaves most like the *standard electrolyte*.
- From an electrochemical point of view both tested co-depositors are a suitable addition to the *standard electrolyte* in a zinc-based secondary battery.
- For both co-depositors, zinc layers deposited from an electrolyte with co-depositor concentrations significantly higher or lower than 0.1 M resulted in zinc layers with significantly more dendrites than there are on zinc layers deposited from an electrolyte containing 0.1 M co-depositor.

Combined improvements

In the previous sections the influence of four different substrates and two different co-depositors on the deposition of zinc from a 1 M $ZnBr_2$ solution is discussed. In Table 1 a summary of the changes in dendrite formation is presented. Thereby the changes in dendrite formation are classified as (=) no change in dendrite formation; (>) increased dendrite formation; (<) decreased dendrite formation. The largest decrease in dendrite formation was observed if (1) the substrate was replaced by a SGL Bipolar substrate, or (2) if 0.1 M of $MgBr_2$ was added to the electrolyte. In both cases no significant change to the electrochemical behaviour in CV was observed. Both replacing the substrate with SGL bipolar graphite and adding 0.1 M of $MgBr_2$ to the electrolyte cause reductions in the dendrite formation. It remains to investigate what the effect will be when both changes are made together; i.e., what the effect will be of depositing a zinc layer from 1 M $ZnBr_2$ + 0.1 M $MgBr_2$ on a SGL bipolar substrate.

In Fig. 8 the morphology of a zinc layer deposited from 1 M $ZnBr_2$ + 0.1 M $MgBr_2$ on a SGL bipolar substrate, and the electrochemical behaviour during this deposition are shown. The voltammogram (Fig. 8b) shows that the electrochemical behaviour of 1 M $ZnBr_2$ + 0.1 M $MgBr_2$ on a SGL bipolar substrate closely resembles the behaviour of the *reference conditions*. In the potential range where zinc deposition occurs, between −0.1 V and −1.5 V, both voltammograms are nearly identical, the largest difference is in the steepness of the peak

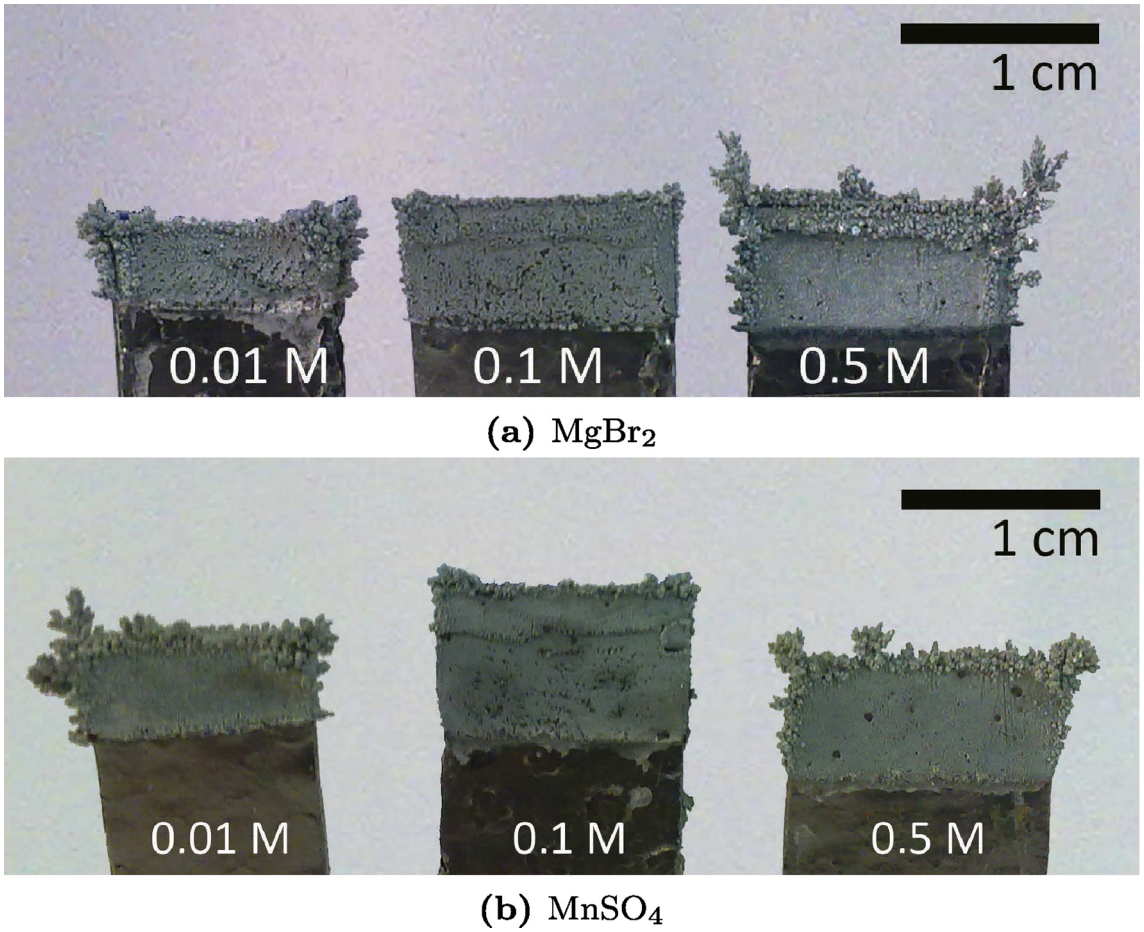

Fig. 7. Morphology of zinc deposited at −1.3 V for 1 h on *standard graphite* from 1 M $ZnBr_2$, with different concentrations of co-depositor.

Table 1
All electrode/ electrolyte combinations tested for this research. (=) No change in dendrite formation; (<) Decreased dendrite formation; (>) Increased dendrite formation.

Substrate	Electrolyte	Additive	Dendrite formation
Reference conditions:			
Standard Graphite	1 M $ZnBr_2$	none	
Varied Substrates			
Sigraflex	1 M $ZnBr_2$	none	<
SGL felt black	1 M $ZnBr_2$	none	=
SGL felt gray	1 M $ZnBr_2$	none	=
SGL Bipolar	1 M $ZnBr_2$	none	≪
Varied Additives			
Standard Graphite	1 M $ZnBr_2$	0.01 M $MgBr_2$	=
Standard Graphite	1 M $ZnBr_2$	0.1 M $MgBr_2$	≪
Standard Graphite	1 M $ZnBr_2$	0.5 M $MgBr_2$	>
Standard Graphite	1 M $ZnBr_2$	0.01 M $MnSO_4$	=
Standard Graphite	1 M $ZnBr_2$	0.1 M $MnSO_4$	<
Standard Graphite	1 M $ZnBr_2$	0.5 M $MnSO_4$	>

at −0.3 V. On the other side of the voltammogram, between −0.1 V and 1.5 V the differences are a bit larger. Both the positive current peak (at 1.5 V) and negative current peak (at 0.3 V) are lower for a deposition form 1 M $ZnBr_2$ + 0.1 M $MgBr_2$ on a SGL bipolar substrate, than for a deposition from *standard electrolyte* on a *standard electrode*. However, as established in Section "Analysis of the reference condition" the behaviour of the electrolyte at the cathode does not significantly influence the behaviour of the electrolyte at the anode. From visual inspection of the electrode (Fig. 8a) it is immediately clear that there are significantly less dendrites than was the case in the *reference conditions*. The deposited zinc layer looks to be even smoother than layers deposited from 1 M $ZnBr_2$ on SGL bipolar graphite substrate or from 1 M $ZnBr_2$ + 0.1 M $MgBr_2$ on *standard graphite* substrate. This combination of the two changes (1 M $ZnBr_2$ + 0.1 M $MgBr_2$ on a SGL bipolar substrate) is referred to as *improved conditions* in the remainder of the paper.

Scanning Electron Microscopy analysis

The morphology of the deposited zinc layer is further analysed using *Scanning Electron Microscopy* (SEM). The SEM analysis was only applied to the improvements that showed the most promising results. This implies that only one substrate is considered: SGL bipolar graphite, in combination with both co-depositors, in addition to the *standard graphite* and *standard electrolyte*.

Firstly the zinc layer deposited from *standard electrolyte* on both substrates is analysed. In both cases zinc was deposited for 1 h at −1.3 V. For the SEM analysis an area on the side of the electrode was selected, where it was immediately clear that zinc had been deposited, but where no dendrite was visible. The image in Fig. 9a shows a zinc layer deposited on a *standard graphite* electrode. In this case, clearly the zinc layer is very terraced, meaning that the thickness of the layer is uneven and in between the portions of different layer thickness there are steep edges. In addition to the variations in layer thickness the distribution over the surface is also uneven, as evidenced by the gaps (black spots) visible in the layer. In Fig. 9b a zinc layer deposited on a *SGL bipolar* electrode is shown. In this case the deposited zinc layer is not terraced. While the thickness of the zinc layer still varies, the transition between areas of different thickness is smooth. There are still some gaps present in the deposited layer, but definitely less than shown in Fig. 9a.

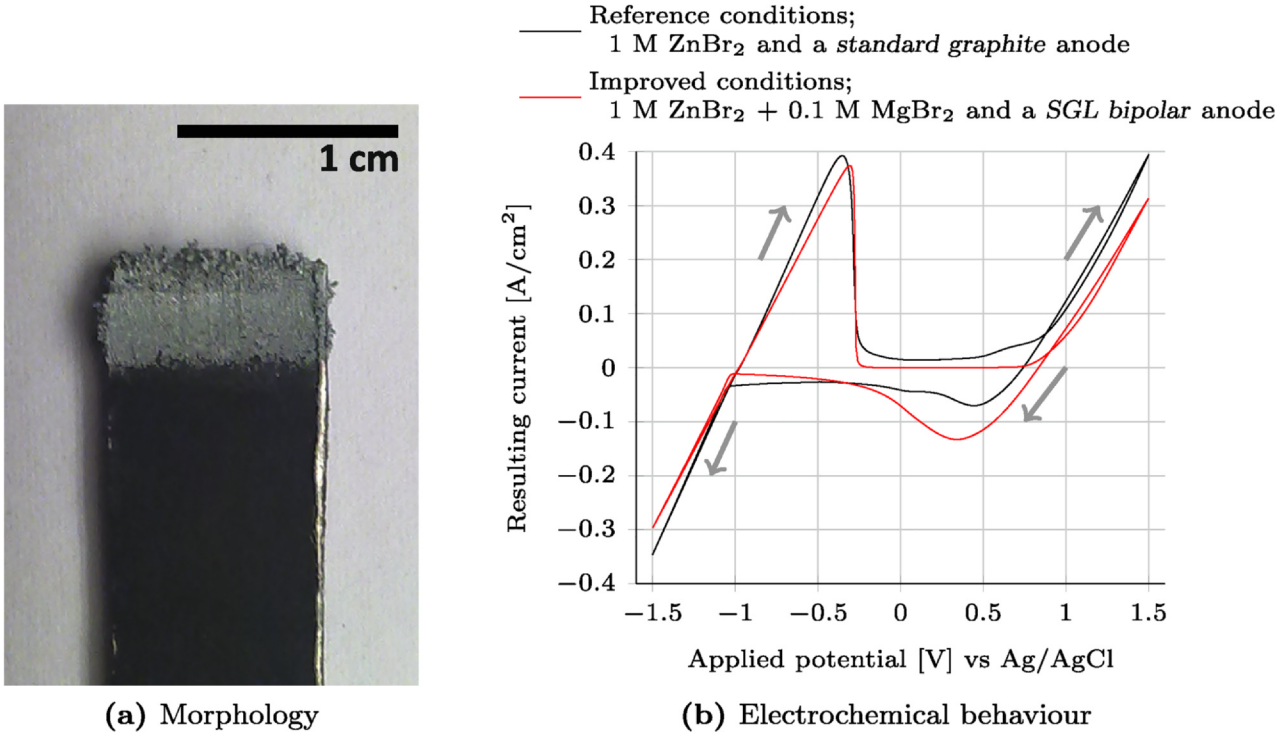

Fig. 8. The morphology of zinc deposited at −1.3 V for 1 h on SGL bipolar graphite from 1 M $ZnBr_2$ + 0.1 M $MgBr_2$ and the corresponding voltammograms showing the elctrochemical behaviour of this deposition, compared to a deposition under *reference conditions*.

Secondly, in Fig. 9c, the zinc layer deposited from 1 M $ZnBr_2$ + 0.1 M $MgBr_2$ on a *standard graphite* electrode is given. As in the previous cases zinc was deposited for 1 h at −1.3 V, and an area on the side of the electrode was selected where it was immediately clear that zinc had been deposited, but where no dendrite was visible. This zinc layer is also somewhat terraced, but clearly less than for the *reference conditions*, indicating that there is less variation in the thickness of the zinc layer than under the *reference conditions* (Fig. 9a). There are again only a few gaps in the layer, indicating that the layer is evenly distributed along the substrate surface.

Lastly the zinc layer deposited under *reference conditions* (Fig. 9a) is compared to the zinc layer deposited under *improved conditions* (Fig. 9d). The zinc layer deposited under *improved conditions* shows very little terracing indicating that there are little hight differences in the zinc layer. Moreover the terracing that does occur is broad, indicating that the hight differences occur gradually. There are very little gaps in the zinc layer, indicating the layer is evenly distributed over the substrate surface.

In conclusion, the zinc layers deposited with one of the two changes (Fig. 9b and c), are smoother and less dendritic than a zinc layer deposited under *standard conditions* (Fig. 9a). A zinc layer with both changes, i.e. deposited under*improved conditions* (Fig. 9d), is even smoother than a zinc layer deposited with only one of the changes applied.

Electrochemical Impedance Spectroscopy analysis

Considering the voltammetry of zinc deposition using the reference conditions and the improved conditions given in Fig. 8b, there is a limited yet clear difference in the voltammetery between a deposition performed using the reference conditions and improved conditions. To make sure that this difference in the voltammetry causes no large differences in the behavior of the battery, a better understanding of the processes occurring at the anode during deposition is needed. In order to gain more insight into the mechanism and kinetics of zinc deposition under the *reference conditions* and *improved conditions* an *Electrochemical Impedance Spectroscopy* (EIS) analysis [40] was performed. Fig. 10 shows the impedance spectra of a deposition under the reference conditions (1 M $ZnBr_2$ on a graphite electrode) and the improved conditions (1 M $ZnBr_2$ + 0.1 M $MgBr_2$ on a bipolar graphite electrode). The EIS measurements were performed during zinc deposition at a potential of −1.3 V (vs Ag/ AgCl), the deposition was started one hour before the EIS measurements were taken to make sure that the system had reached a steady state before the start of the measurements.

Fig. 10a displays the impedance spectrum of the EIS measurements on the zinc deposition under *standard conditions*. The offset of the spectrum on the x-axis at ~ 1.1 Ω is associated with the resistance of the electrolyte; the higher the offset of the spectrum, the higher the internal resistance of the electrolyte. The width of the spectrum, in this case approximately 2.5 Ω, is associated with the charge transfer resistance. The relatively large charge transfer resistance is attributed to the crystallization processes and the relatively large over potential (−1.3 V) applied to drive the deposition. The impedance spectrum of the deposition under *improved conditions* is displayed in Fig. 10b. In this case the offset of the graph is approximately 1.2 Ω, which is slightly larger than that of the *standard conditions*. The slightly higher electrolyte resistance may be related to the presence of magnesium ions in the electrolyte of the *improved condition*.

In order to understand the impedance spectra on a more detailed level the data was fitted using the equivalent circuit processing software (*EQUIVCRT*) and the method developed by Boukamp [38,39]. The fitted impedance spectra are also displayed in Fig. 10a and b. The fitted spectra are nearly identical to the measured spectra. The residual error between the fitted data and the measured data is displayed in Fig. 10c and d. It stayed within 0.1% over a wide range of frequencies, however larger errors were encountered at very high frequencies[3]. The equivalent circuit fitted using the *EQUIVCRT* software is displayed in Fig. 11.

The best fitted equivalent circuit (see Fig. 11a) is relatively simple, consisting of three resistors (R, R_4, and R_2), a capacitor (C) and a

[3] Note that small numbers in the impedance spectra correspond to large frequencies in the residual error plots.

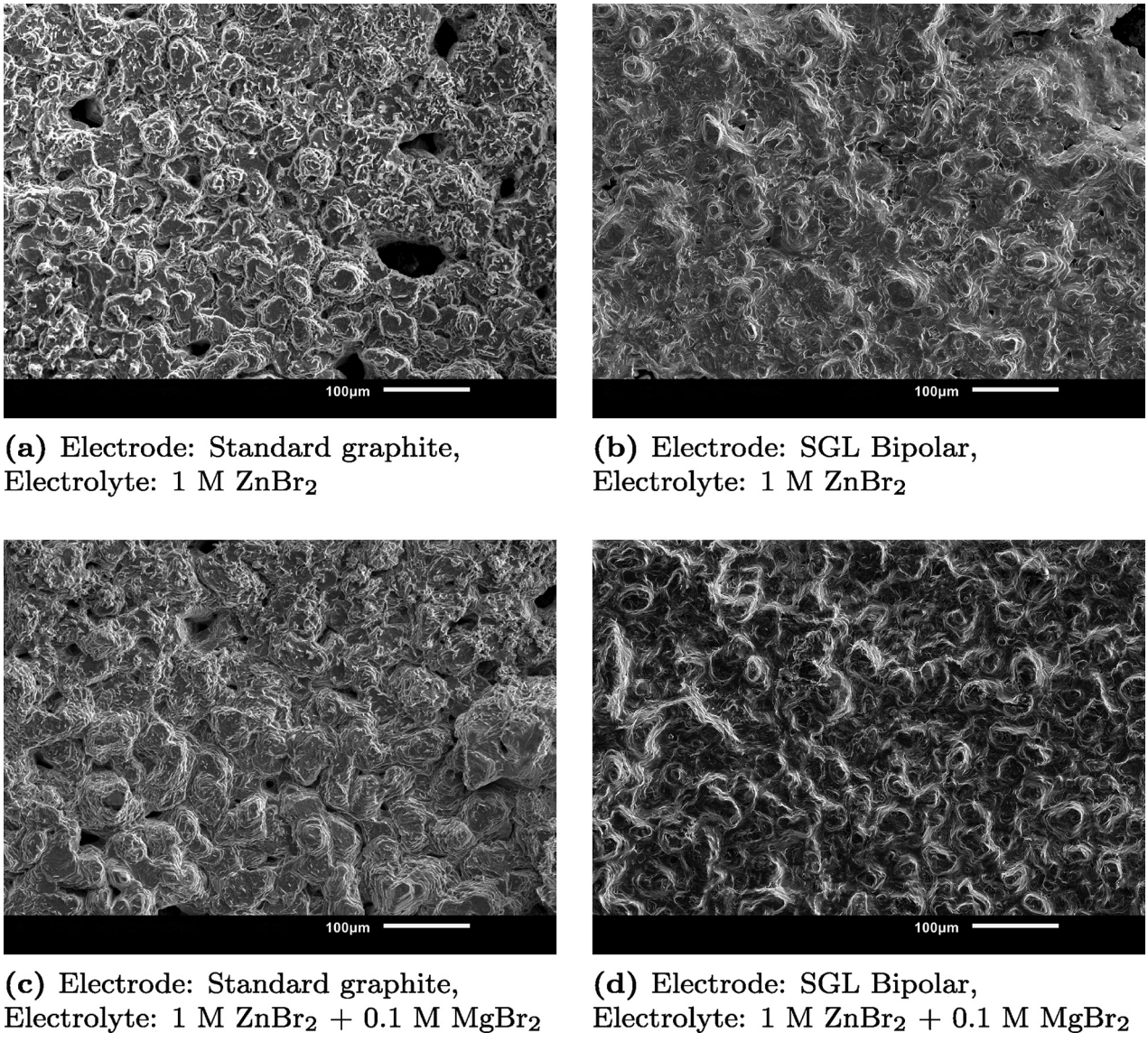

(a) Electrode: Standard graphite, Electrolyte: 1 M $ZnBr_2$

(b) Electrode: SGL Bipolar, Electrolyte: 1 M $ZnBr_2$

(c) Electrode: Standard graphite, Electrolyte: 1 M $ZnBr_2$ + 0.1 M $MgBr_2$

(d) Electrode: SGL Bipolar, Electrolyte: 1 M $ZnBr_2$ + 0.1 M $MgBr_2$

Fig. 9. Scanning Electron Microscope pictures of the various zinc layers, recorded with a 200× magnification.

constant phase element (Q). Resistor R corresponds to the electrolyte resistance, and resistor R_4 corresponds to the charge transfer resistance. The values fitted for R and R_4 (see Fig. 11b) are nearly identical to the values obtained for both cases from the impedance spectra (see Fig. 10). The parallel setting of resistance R_2 and constant phase element Q may be associated with diffusion. The values for R_2 and Q are very small for both the reference conditions and improved conditions, indicating that the zinc deposition is controlled by diffusion of ions towards the substrate surface and by adsorption at the substrate surface via a weak *Van der Waals* bond [41]. The small value for C, present in both the *reference condition* and the *improved condition*, indicates that during the deposition process electrolyte is likely enclosed in the pores of the substrate surface.

In conclusion, the impedance spectra for the reference conditions and improved conditions are very similar, whereby the differences in the offset and width of the curve are attributed to the differences in the electrolyte. Both spectra can be fitted to the same equivalent circuit (Fig. 11), with slightly different values for all components. The presence of the elements and the corresponding values for both the reference conditions and improved conditions, suggest a deposition process dominated by diffusion towards the surface of the carbon electrode and by heterogeneous nucleation.

Conclusion

Dendrite formation during the electrochemical deposition of zinc can cause problems in the operation of a zinc-based secondary battery. Any practical solution to this problem should not have (negative) influence on the operation of the zinc-based secondary battery as a whole, meaning that the behaviour of the electrolyte at the anode should be the same in all cases whether the practical solution is applied or not.

To get some more insight, the deposited zinc layers were analysed using optical microscopy as well as scanning electron microscopy. And the behaviour of the electrolyte at the anode was analysed using cyclic voltammetry. Firstly, various substrates, which are possible replacements for the substrate used in the *standard conditions*, were researched. The used electrode materials all have little influence on the behaviour of the electrolyte at the anode. Hereby, the SGL bipolar graphite shows the least dendrite formation of all tested substrates. Secondly, the addition of several co-depositor materials to the electrolyse has been researched. As with the substrate, for a practical solution, the co-depositor should have as little influence as possible on the behaviour of the electrolyte at the anode. It is demonstrated that the addition of 0.1 M $MgBr_2$ to the electrolyte causes a significant reduction of the formation of dendrites, while the behaviour of the electrolyte at the

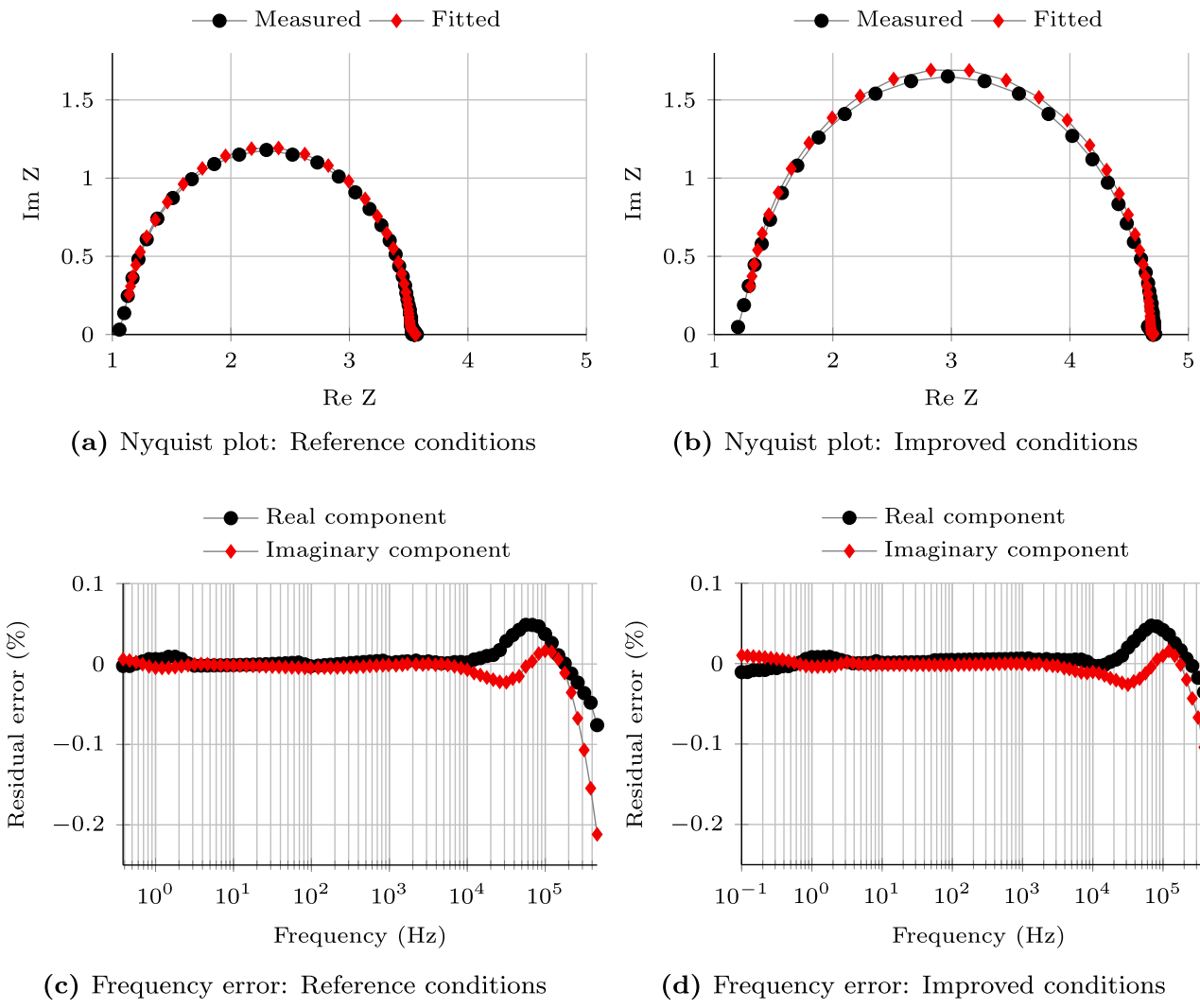

(a) Nyquist plot: Reference conditions

(b) Nyquist plot: Improved conditions

(c) Frequency error: Reference conditions

(d) Frequency error: Improved conditions

Fig. 10. Impedance spectra and residual error plots for EIS measurements of zinc depositions under *reference conditions* and *improved conditions* and fitted using the EQUIVCRT software and circuit in Fig. 11.

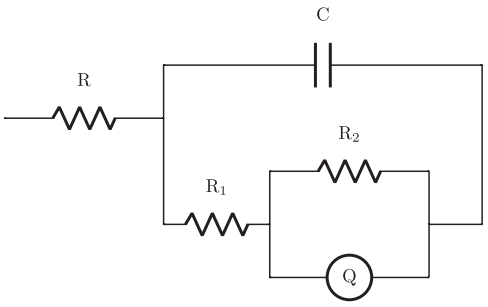

(a)

	Reference condition	Improved condition
Substrate	Standard graphite	SGL Bipolar
Electrolyte	1M $ZnBr_2$	1M $ZnBr_2$ + 0.1M $MgBr_2$
$\mathbf{U_{applied}}$ **(V)**	-1.3	-1.3
R (Ω)	1.11	1.28
C (F)	$1.33{\cdot}10^{-6}$	$9.09{\cdot}10^{-7}$
$\mathbf{R_1}$ (Ω)	2.39	2.44
$\mathbf{R_2}$ (Ω)	$5.46{\cdot}10^{-2}$	$7.50{\cdot}10^{-1}$
Q (F)	$1.49{\cdot}10^{-1}$	$3.22{\cdot}10^{-1}$
n (-)	$6.75{\cdot}10^{-1}$	$9.99{\cdot}10^{-3}$

(b)

Fig. 11. (a) Equivalent circuit representing the processes likely to occur during zinc deposition and (b) values of the elements in the circuit for both the reference and improved conditions.

anode is influenced very little. Furthermore, it is demonstrated experimentally that both solutions combined (*improved conditions*), result in a further reduction of dendrite formation.

Lastly, an electrochemical impedance spectroscopy study was conducted on the deposition using both the *reference conditions* and *improved conditions*. It is shown that the deposition under both sets of conditions is a process likely dominated by heterogeneous nucleation. The processes are slightly different, yet sufficiently similar to ensure that the deposition under the *improved conditions* does not (negatively) influence the overall working of the zinc-based secondary battery as a whole.

Summarizing, it has been demonstrated that the formation dendrites at the anode of a zinc-based secondary battery can be reduced by using an SGL graphite anode or adding 0.1 M $MgBr_2$ to the electrolyte, and it

has been demonstrated that both measures have no (negative) influence on the over-all working of the battery.

Future work

Future work should be dedicated to better the understanding of both deposition processes. An in-depth EIS study of the deposition process under both the *reference conditions* and *improved conditions* and an analysis of the over-potential during deposition could prove to be valuable for this understanding. Furthermore a study on the deposited layer using analysis techniques like *X-ray diffraction Atomic Force Microscopy Energy Dispersive X-ray spectroscopy* and *Crystallography*would definitely shed more light on the surface morphology and exact composition of the deposited layers. Additionally, an analysis of cross-sections of deposited zinc layers, in various states of development, could improve our understanding of the mechanics of dendrite growth and the influence of the various substrates and additives on these mechanics. Lastly, future work should also be dedicated to applying the solutions presented in this paper to a practical zinc-based secondary battery, more specifically to improve the *Seasalt Battery* currently in development at the company Dr. Ten B.V.

CRediT authorship contribution statement

Bart Homan: Investigation, Validation, Formal analysis, Visualization, Writing - original draft. **Diego F. Quintero Pulido:** Methodology, Formal analysis, Writing - review & editing. **Marnix V. ten Kortenaar:** Conceptualization, Supervision, Resources, Funding acquisition. **Johann L. Hurink:** Supervision, Project administration, Writing - review & editing. **Gerard J.M. Smit:** Supervision, Writing - review & editing.

Declaration of Competing Interest

The authors declare that they have no known competing financial interests or personal relationships that could have appeared to influence the work reported in this paper.

Acknowledgements

The authors thank Dr. Ten B.V., the Dutch ministry for Economic affairs, the Dutch organisation Rijksdienst voor Ondernemend Nederland (program: *"Energie Onderzoek Subsidie"*) and professor Roberto Balda Ayala at the La Salle University in Colombia, for their support. The authors would also like to acknowledge the anonymous reviewers for their constructive comments on this work. Lastly, the authors extend special thanks to Rajat Bhardwaj at the Delft University of Technology, for his invaluable help in performing the *scanning electron microscopy* analysis.

Appendix A. Supplementary data

Supplementary data associated with this article can be found, in the online version, athttps://doi.org/10.1016/j.seta.2020.100820.

References

[1] Roberts BP, Sandberg C. The role of energy storage in development of smart grids. Proc IEEE 2011;99(6):1139–44. https://doi.org/10.1109/jproc.2011.2116752.
[2] Wong LA, Ramachandaramurthy VK, Taylor P, Ekanayake JB, Walker SL, Padmanaban S. Review on the optimal placement, sizing and control of an energy storage system in the distribution network. J Energy Storage 2019;21:489–504. https://doi.org/10.1016/j.est.2018.12.015.
[3] Baumann M, Weil M, Peters JF, Chibeles-Martins N, Moniz AB. A review of multi-criteria decision making approaches for evaluating energy storage systems for grid applications. Renew Sustain Energy Rev 2019;107:516–34. https://doi.org/10.1016/j.rser.2019.02.016.
[4] USGS. Mineral commodity summaries 2020: U.S. Geological Survey. 2020. ISBN 978-1-4113-4362-7.https://doi.org/10.3133/mcs2020.
[5] Kesler S, Simon A. Mineral Resources, Economics and the Environment. Cambridge University Press978-13-16368-58-9; 2015.
[6] Statista. [Online] Available:https://statista.com; 2020. Last accessed on 7-1-2020.
[7] Edited by: van Leeuwen P., van de Leur B. Chemiekaarten, chemical compound information database. 2019. Last accessed on 1-9-2019.
[8] Chen L, Xu Z, Liu M, Huang Y, Fan R, Su Y, et al. Lead exposure assessment from study near a lead-acid battery factory in china. Sci Total Environ 2012;429:191–8. https://doi.org/10.1016/j.scitotenv.2012.04.015.
[9] Gottesfeld P, Were F, Adogame L, Gharbi S, San D, Nota M, et al. Soil contamination from lead battery manufacturing and recycling in seven african countries. Environ Res 2018;161:609–14. https://doi.org/10.1016/j.envres.2017.11.055.
[10] Mclarnon FR, Cairns EJ. The secondary alkaline zinc electrode. J Electrochem Soc 1991;138(2):645–6. https://doi.org/10.1149/1.2085653.
[11] Pelt W. Zinc/Bromine battery electrolytes: electrochemical, physico-chemical and spectroscopic studies. Ph.D. thesis; University of Ottawa; 1994.
[12] Quintero Pulido DF, ten Kortenaar MV, Hurink JL, Smit GJM. Characteristics of halide oxidation at graphite electrode for use in halde batteries. Sustain Energy Technol Assessments 2019;33:14–23. https://doi.org/10.1016/j.seta.2019.03.001.
[13] Quintero Pulido DF. Energy storage technologies for off-grid houses. Ph.D. thesis; University of Twente; 2019.https://doi.org/10.3990/1.9789036548267.
[14] Lu W, Xie C, Zhang H, Li X. Inhibition of zinc dendrite growth in zinc-based batteries. ChemSusChem 2018;11:3996–4006. https://doi.org/10.1002/cssc.201801657.
[15] Palacín MR, de Guilbert A. Why do batteries fail? Science 2016;315(6273):574. https://doi.org/10.1126/science.1253292.
[16] Grier D, Ben-Jacob E, Clarke R, Sander LM. Morphology and microstructure in electrochemical deposition of zinc. Phys Rev Lett 1986;56(12):1264–7. https://doi.org/10.1103/physrevlett.56.1264.
[17] Muralidhara HB, Arthoba Naik Y. Electrochemical deposition of nanocrystalline zinc on steel substrate from acid zincate bath. Surf Coat Technol 2008;202:3403–12. https://doi.org/10.1016/j.surfcoat.2007.12.012.
[18] Fukami K, Nakanishi S, Yamasaki H, Tada T, KS, Kamikawa N, et al. General mechanism for the synchronization of electrochemical oscilations and self-organized dendrite electrodeposition of metals with ordered 2d and 3d microstructures. J Phys Chem C 2007;111:1150–1160.https://doi.org/10.1021/jp063462t.
[19] Fukami K, Nakanishi S, Tada T, Yamasaki H, Sakai S, Fukushima S, et al. Self-organized periodic growth of stacked hexagonal wafers in synchronization with a potential oscillation in zinc electrodeposition. J Electrochem Soc 2004;152(7):C493–7. https://doi.org/10.1149/1.1932829.
[20] Shitanda I, Ichikawa R, Hosh Y, Itagaki M. A vegetable garden-like zinc dendritic patterning by electrodeposition. Chem Soc Jpn 2014;43:113–5. https://doi.org/10.1246/cl.130921.
[21] Koda R, Fukami K, Sakka T, Ogata YH. A physical mechanism for suppression of zinc dendrites caused by high efficiency of the electrodeposition within confined nanopores. ECS Electrochem Lett 2013;2(2):D9–11. https://doi.org/10.1149/2.010302eel.
[22] Gomes A, da Silva Pereira MI. Pulsed electrodeposition of Zn in the presence of surfactants. Electrochim Acta 2006;51:1342–50. https://doi.org/10.1016/j.electacta.2005.06.023.
[23] Gomes A, da Silva Pereira MI. Zn electrodeposition in the presence of surfactants Part I. Voltammetric and structural studies. Electrochim Acta 2006;52:863–71. https://doi.org/10.1016/j.electacta.2006.06.025.
[24] Raeissi K, Saatchi A, Golozar MA, Szpunar JA. Texture and surface morphology in zinc electrodeposits. J Appl Electrochem 2004;34:1249–58. https://doi.org/10.1007/s10800-004-1699-8.
[25] Boiadjieva T, Monev M, Tomandl A, Kronberger H, Fafilek G. Electrochemical studies on Zn deposition and dissolution in sulphate electrolyte. J Solid State Electrochem 2009;13:671–7. https://doi.org/10.1007/s10008-008-0594-3.
[26] Zhang SY, Li Q, Chen B, Xu SQ, Fan JM, Luo F. Electrodeposition of zinc on AZ91D magnesium alloy pre-treated by stannate conversion coatings. Mater Corros 2010;61(10):860–5. https://doi.org/10.1002/maco.200905435.
[27] Ferapontova EE, Terry JG, Walton AJ, Mountford CP, Crain J, Buck AH, et al. Electrochemical deposition of Zn on TiN microelectrode arrays for microanodes. Electrochem Commun 2007;9:303–9. https://doi.org/10.1016/j.elecom.2006.09.005.
[28] Granados-Neria M, Mendoza Huizar LH, Rios-Reyes CH. Electrochemical study about zinc electrodeposition onto gce and hopgg substrates. Quimica Nova 2011;34(3):439–43. https://doi.org/10.1590/s0100-40422011000300014.
[29] Raeissi K, Saatchia A, Golozara MA, Szpunar JA. Effect of surface preparation on zinc electrodeposited texture. Surf Coat Technol 2005;197:229–37. https://doi.org/10.1016/j.surfcoat.2004.09.024.
[30] Gao X, Wu H, Li W, Tian Y, Zhang Y, Wu H, et al. H+ insertion boosted α-mno2 for an aqueous zn-ion battery. Small 2020;16:1905842. https://doi.org/10.1002/smll.201905842.
[31] Vasilache V, Gutt G, Vasilache T. Studies about electrochemical plating with zinc - nickel alloys- the influence of deposition potential on stoichiometric composition. Revista de Chimie 2008;59(9):1005–8.
[32] Foyet A, Hauser A, Schaefer W. Template electrochemical deposition and characterization of zinc-nickel alloy nanomaterial. J Elecroanal Chem 2007;604(2):137–43. https://doi.org/10.1016/j.jelechem.2007.03.014.
[33] Musa AY, Kadhum AAH, Takriff MS, Slaiman QJM. Co-deposition of copper-zinc alloy in cyanide-based electrolytes. Int J Surf Sci Eng 2008;2(6):541–9. https://doi.org/10.1504/ijsurfse.2008.022290.
[34] Olesen PT, Steenberg T, Christensen E, Bjerrum NJ. Electrolytic deposition of amorphous and crystalline zinc-calcium phosphates. J Mater Sci

1998;33(12):3059–63. https://doi.org/10.1023/a:1004379319348.
[35] Abbott AP, Barron JC, Frisch G, Ryder KS, Silva AF. The effect of additives on zinc electrodeposition from deep eutectic solvents. Electrochim Acta 2011;56:5272–9. https://doi.org/10.1016/j.electacta.2011.02.095.
[36] Li M, Luo S, Qian Y, Zhang W, Jiang L, Shena J. Effect of additives on electrodeposition of nanocrystalline zinc from acidic sulfate solutions. J Electrochem Soc 2007;154(11):D567–71. https://doi.org/10.1149/1.2772093.
[37] Ortiz-Aparicio JL, Meas Y, Trejo G, Ortega R, Chapman TW, Chainet E. Effects of organic additives on zinc electrodeposition from alkaline electrolytes. J Appl Electrochem 2013;43:289–300. https://doi.org/10.1007/s10800-012-0518-x.
[38] Boukamp BA. A nonlinear least squares fit procedure for analysis of immittance data of electrochemical systems. Solid State Ionics 1986;20:31–44. https://doi.org/10.1016/0167-2738(86)90031-7.
[39] Boukamp BA. Package for impedance/admittance data analysis. Solid State Ionics 1986;19:136–40. https://doi.org/10.1016/0167-2738(86)90100-1.
[40] Lasia A. Electrochemical Impedance Spectroscopy and its Applications. Springer; 2014.https://doi.org/10.1007/978-1-4614-8933-7.
[41] Alias N, Mohamad AA. Morphology study of electrodeposited zinc from zinc sulfate solutions as anode for zinc-air and zinc-carbon batteries. J King Saud Univ Eng Sci 2015;27:43–8. https://doi.org/10.1016/j.jksues.2013.03.003.